Indian J. pure appl. Math., 31(10) : 1317-1337, October 2000

WAVE PROPAGATION IN MICROPOLAR LIQUID-SATURATED POROUS SOLID

RAJNEESH KUMAR* AND SUNITA DESWAL**

*Department of Mathematics, Kurukshetra University, Kurukshetra 136 119, Haryana, India

**Department of Mathematics, Fateh Chand College for Women, Hisar 125 001, Haryana, India

The present investigation is concerned with wave propagation in a liquid-saturated porous solid with micropolar elastic skeleton. Two different cases have been discussed — (i) Reflection of micropolar elastic waves at the free surface of a micropolar elastic liquid-saturated porous solid; and (ii) Propagation of Rayleigh waves in a micropolar elastic liquid-saturated porous solid. In case (i), the amplitude ratios for the different reflected waves have been calculated and presented graphically for different angles of emergence. Some special cases have been deduced. In case (ii), the frequency equation is derived and dispersion curves giving phase velocity as a function of frequency ratio and normalized wave number have been plotted graphically for a particular model.

Key Words : Wave Propagation; Micropolar Liquid-Saturated Porous Solid; Frequency Ratio; Frequency Equation; Rayleigh Waves

INTRODUCTION

Dynamic analysis of liquid-saturated porous media is a subject with applications in numerous branches of science and engineering, including geophysics, seismology, civil and mechanical engineering. Liquid-saturated porous materials are often present on and below the surface of the earth in the form of sandstone, limestone and other sediments permeated by groundwater or oil. Biot[1&2] studied the propagation of plane harmonic seismic waves in liquid-saturated porous solids. Biot[3] presented a unified treatment of the mechanics of deformation and acoustic propagation in porous media. He treated the liquid-solid medium as a complex physico-chemical system with resultant relaxation and viscoelastic properties. Deresiewicz[4] and Deresiewicz and Rice[5] studied the reflection at the plane traction-free surface of non-dissipative and dissipative liquid-saturated porous solids respectively.

The discrepancy between the results of classical theory of elasticity and the experiments appear in all cases when the microstructure of the body is significant i.e., in the neighbourhood of cracks and notches where the stress gradients are considerable. The discrepancies also appear in granular media and multimolecular bodies such as polymers. The influence of the microstructure is particularly evident in the case of elastic vibrations of high frequency and small wave length. Eringen and Suhubi[6] introduced theories of micropolar elastic solids in which the micromotions of the particle contained in a macro volume element with respect to its centroid are considered. Materials which are affected by such micromotions and macrodeformations are known as micromorphic materials[7]. Eringen[8] developed a theory for a subclass of micromorphic materials which are called micropolar media and these materials show microrotation's effect and microrotational inertia.

Recent experiments by Gauthier[11] reveal that the micropolar wave can be excited and detected in typical solids. Yang and Lakes[19] suggest with a reasonable degree of confidence that human bone can adequately be used as a model for theory of micropolar elasticity. Many researchers[16 & 17

studied the problem of wave propagation at poroelastic solid interface. The behaviour of plane harmonic waves propagating in a liquid-saturated viscoelastic porous media with micropolar skeleton was studied by Konczak[13]. Konczak[12] also worked on thermo-mechanical effects on liquid-saturated porous viscoelastic media with a micropolar skeleton. Inspite of these studies, not much work has been done on wave propagation in micropolar liquid saturated porous media. We make an attempt to study the wave propagation in micropolar liquid-saturated porous half space.

GEOMETRY OF THE PROBLEM

We consider the micropolar liquid-saturated porous solid half space V and introducing r ngular Cartesian co-ordinate system OXYZ such that $z = 0$ represents the equation of the free s' e and the z-axis is directed into the medium as shown in Fig. 1.

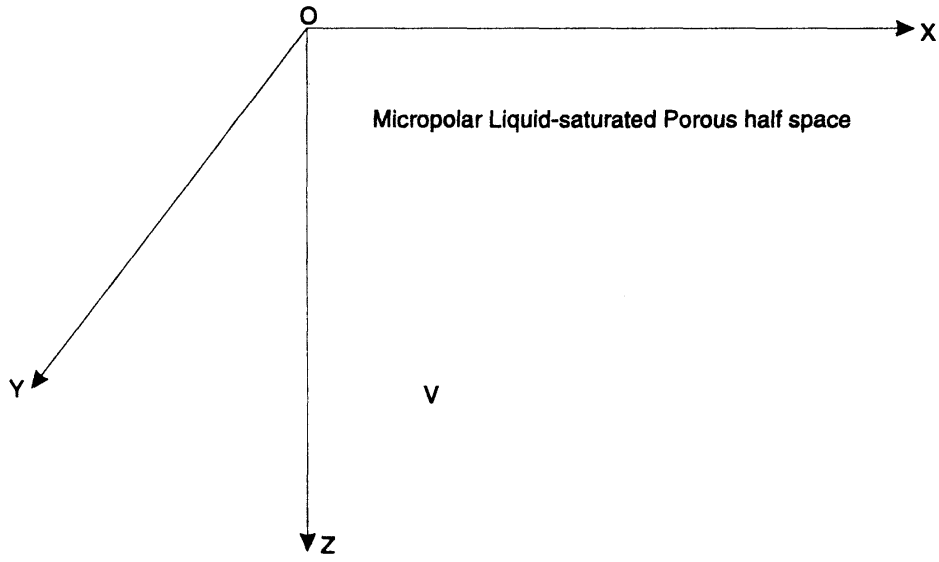

FIG. 1

BASIC EQUATIONS AND SOLUTION OF THE PROBLEM

Following Eringen[9] and Konczak[12, 13] the field equations for a micropolar liquid-saturated porous solid in the presence of dissipation are given by —

$$(\lambda+2\mu+K)\,\nabla(\nabla\cdot\boldsymbol{u})-(\mu+K)\,\nabla\times(\nabla\times\boldsymbol{u})+K\,\nabla\times\boldsymbol{\phi}+Q\,\nabla(\nabla\cdot\boldsymbol{U})$$

$$=\frac{\partial^2}{\partial t^2}(\rho_{11}\boldsymbol{u}+\rho_{12}\boldsymbol{U})+b\frac{\partial}{\partial t}(\boldsymbol{u}-\boldsymbol{U}), \qquad \ldots (1)$$

$$\text{grad}\,(Qe+R\,\varepsilon)=\frac{\partial^2}{\partial t^2}(\rho_{12}\boldsymbol{u}+\rho_{22}\boldsymbol{U})-\frac{b\,\partial}{\partial t}(\boldsymbol{u}-\boldsymbol{U}) \qquad \ldots (2)$$

and $$(\alpha+\beta+\gamma)\,\nabla(\nabla\cdot\boldsymbol{\phi})-\gamma\,\nabla\times(\nabla\times\boldsymbol{\phi})+K(\nabla\times\boldsymbol{u})-2K\boldsymbol{\phi}=\rho j\frac{\partial^2\boldsymbol{\phi}}{\partial t^2}, \quad \ldots (3)$$

where $\lambda, \mu, K, \alpha, \beta, \gamma$ are material constants for the solid-liquid aggregate, ρ is the density of the medium and j is the microinertia. $\boldsymbol{u}$ and $\boldsymbol{U}$ are the displacements in the solid and liquid parts, respectively and e = div $\boldsymbol{u}$, ε = div $\boldsymbol{U}$ are the corresponding dilatations; $\boldsymbol{\phi}$ is the microrotation vector. Q is a measure of coupling between the volume change of the solid and of the liquid. R is a measure of the pressure that must be exerted on the fluid to force a given volume of it into the aggregate while total volume remains constant. $\rho_{11}, \rho_{12}, \rho_{22}$ are dynamical co-efficients and b is a dissipation function.

Assuming time harmonic variations ($e^{i\omega t}$) and considering the Helmhtz resolution of displacement vectors as

$$\boldsymbol{u} = \text{grad } q + \text{curl } \boldsymbol{H}, \quad \ldots (4)$$

and

$$\boldsymbol{U} = \text{grad } \boldsymbol{\psi} + \text{curl } \boldsymbol{G}$$

and then eliminating ψ, $\nabla^2\psi$, ϕ_2 and $\nabla^2\phi_2$ from the resulting expressions, we obtain the following equations

$$(A\nabla^4+B\omega^2\nabla^2+\omega^4 C)\,q=0, \quad \ldots (5)$$

$$[A\nabla^2+\omega^2(R\rho_{11}-\rho_{12}Q)+i\omega b(R+Q)]\,q-\omega^2 B'\psi=0, \quad \ldots (6)$$

$$(\nabla^4+D\omega^2\nabla^2+E\omega^4)\,H^*=0, \quad \ldots (7)$$

and

$$\nabla^2(\nabla^2+\omega^2 E_2+pr_2)\,H^*-p[-r_0+r_1\omega^2]\,\phi_2=0, \quad \ldots (8)$$

where

$$H^*=(-\boldsymbol{H})_y,\ \phi_2=(-\boldsymbol{\phi})_y,$$

$$A=PR-Q^2,\ P=\lambda+2\mu+K,\ p=\frac{K}{\mu+K},$$

$$B=P\left(\rho_{22}+\frac{ib}{\omega}\right)+R\left(\rho_{11}+\frac{ib}{\omega}\right)-2Q\left(\rho_{12}-\frac{ib}{\omega}\right),$$

$$C=\left(\rho_{11}+\frac{ib}{\omega}\right)\left(\rho_{22}+\frac{ib}{\omega}\right)-\left(\rho_{12}-\frac{ib}{\omega}\right)^2,$$

$$B'=(\rho_{22}Q-\rho_{12}R)+\frac{ib}{\omega}(R+Q),$$

$$D = E_2 + r_1 + \frac{(pr_2 - r_0)}{\omega^2},\ r_2 = \frac{K}{\gamma},$$

$$E = E_2\left(r_1 - \frac{r_0}{\omega^2}\right),\ E_2 = \frac{E_1}{\mu + K},\ r_0 = \frac{2K}{\gamma},\ r_1 = \frac{\rho j}{\gamma},$$

and

$$E_1 = \left[\rho_{11} + \rho_{12}\frac{-\rho_{12}\,\omega + ib}{\rho_{22}\,\omega + ib} + ib\frac{\rho_{22} + \rho_{12}}{\rho_{22}\,\omega + ib}\right]. \qquad ...(9)$$

We assume the solution of eq. (5) as

$$q = q_1^* + q_2^*, \qquad ... (10)$$

where q_1^* and q_2^* satisfy

$$(\nabla^2 + \delta_1^2)\,q_1^* = 0 \text{ and } (\nabla^2 + \delta_2^2)\,q_2^* = 0, \qquad ... (11)$$

where

$$\delta_1^2 = \lambda_1^2\,\omega^2,\ \delta_2^2 = \lambda_2^2\,\omega^2, \qquad ... (12)$$

$$\lambda_1^2,\ \lambda_2^2 = [B \mp (B^2 - 4AC)^{1/2}]/2A. \qquad ... (13)$$

Hence in an unbounded medium solution of eq. (11) corresponds to two coupled longitudinal waves. The wave corresponding to q_1^* being the faster one, called fast longitudinal displacement wave (or P_f) wave propagating with the phase velocity λ_1^{-1} and that corresponding to q_2^* being the slower one, called slow longitudinal displacement (or P_s) wave propagating with the phase velocity λ_2^{-1}.

With the help of eqs. (10-13), we have from eq. (6)

$$\psi = \mu_1\,q_1^* + \mu_2\,q_2^*, \qquad ... (14)$$

where

$$\mu_{1,2} = \frac{1}{B'}\left[-A\,\lambda_{1,2}^2 + (\rho_{11}\,R - \rho_{12}\,Q) + \frac{ib}{\omega}(R + Q)\right]. \qquad ... (15)$$

Taking the solution of eq. (7) as

$$H^* = H_1^* + H_2^*, \qquad ... (16)$$

where H_1^* and H_2^* satisfy

$$(\nabla^2 + \delta_3^2)\, H_1^* = 0,\ (\nabla^2 + \delta_4^2)\, H_2^* = 0, \qquad \ldots (17)$$

where

$$\delta_{3,4}^2 = \omega^2 \lambda_{3,4}^2\ ,\ \lambda_{3,4}^2 = [D \mp (D^2 - 4E)^{1/2}]/2. \qquad \ldots (18)$$

Using eqs. (16), (17) and (18) in eq. (8), we get

$$\phi_2 = \mu_3 H_1^* + \mu_4 + H_2^*, \qquad \ldots (19)$$

where

$$\mu_{3,4} = \frac{\delta_{3,4}^2 (\delta_{3,4}^2 - \omega^2 E_2 - pr_2)}{p[-r_0 + r_1 \omega^2]}. \qquad \ldots (20)$$

In an unbounded medium the solutions of eq. (17) correspond to two coupled transverse and microrotational waves propagating with velocities λ_3^{-1} and λ_4^{-1}.

Following Eringen[9] and Konczak[12&13] the stress-strain relations are given as

$$t_{kl} = (\lambda u_{r,r} + Q U_{r,r})\, \delta_{kl} + \mu [u_{k,l} + u_{l,k}] + K [u_{l,k} - \varepsilon_{klr} \phi_r],$$

$$m_{kl} = \alpha \phi_{r,r}\, \delta_{kl} + \beta \phi_{k,l} + \gamma \phi_{l,k}$$

and $$\sigma = Qe + R \varepsilon. \qquad \ldots (21)$$

BOUNDARY CONDITIONS

The boundary conditions at the free surface (i.e., $z = 0$), are the vanishing of normal force stress, tangential force stress, tangential couple stress and normal stress in liquid; that is

$$t_{zz} = t_{zx} = m_{zy} = \sigma = 0, \text{ at } z = 0. \qquad \ldots (22)$$

Case I — Reflection at the Free Surface.

We consider micropolar elastic waves [coupled longitudinal (P_f and P_s) and coupled transverse and microrotational wave], propagating through the micropolar liquid-saturated porous elastic half space and incident at the free surface $z = 0$, with the direction of propagation making an angle θ_0 with the free surface. Corresponding to the incident wave, we get reflected P_f wave, P_s wave and a set of two coupled transverse and microrotational waves as shown in Fig. 1(*a*).

The potential functions satisfying the boundary conditions (22) are

$$q = A_1 \exp [i\delta_1 (x \cos \theta_0 - z \sin \theta_0) - i\omega_1 t] +$$

$$B_1 \exp [i\delta_1 (x \cos \theta_1 + z \sin \theta_1) - i\omega_1 t] +$$

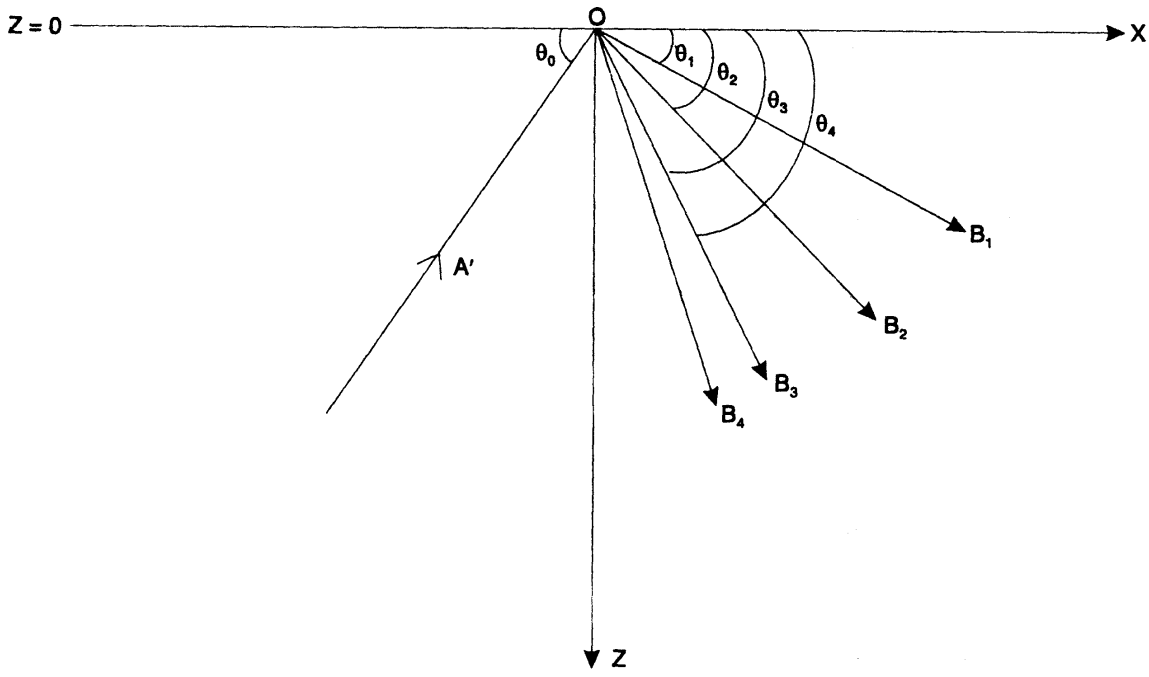

FIG. 1(a)

$$A_2 \exp\,[i\delta_2\,(x\cos\theta_0 - z\sin\theta_0) - i\omega_2 t] +$$

$$B_2 \exp\,[i\delta_2\,(x\cos\theta_2 + z\sin\theta_2) - i\omega_2 t]\ ,$$

$$\psi = \mu_1 A_1 \exp\,[i\delta_1\,(x\cos\theta_0 - z\sin\theta_0) - i\omega_1 t] +$$

$$\mu_1 B_1 \exp\,[i\delta_1\,(x\cos\theta_1 + z\sin\theta_1) - i\omega_1 t] +$$

$$\mu_2 A_2 \exp\,[i\delta_2\,(x\cos\theta_0 - z\sin\theta_0) - i\omega_2 t] +$$

$$\mu_2 B_2 \exp\,[i\delta_2\,(x\cos\theta_2 + z\sin\theta_2) - i\omega_2 t],$$

$$H^* = A_4 \exp\,[i\delta_4\,(x\cos\theta_0 - z\sin\theta_0) - i\omega_4 t] +$$

$$B_4 \exp\,[i\delta_4\,(x\cos\theta_4 + z\sin\theta_4) - i\omega_4 t] +$$

$$B_3 \exp\,[i\delta_3\,(x\cos\theta_3 + z\sin\theta_3) - i\omega_3 t],$$

$$\phi_2 = \mu_4 A_4 \exp\,[i\delta_4\,(x\cos\theta_0 - z\sin\theta_0) - i\omega_4 t] +$$

$$\mu_4 B_4 \exp\,[i\delta_4\,(x\cos\theta_4 + z\sin\theta_4) - i\omega_4 t] +$$

$$\mu_3 B_3 \exp\,[i\delta_3\,(x\cos\theta_3 + z\sin\theta_3) - i\omega_3 t] \qquad \ldots (23)$$

where $A_2, A_4 = 0$, for incident P_f wave,

$A_1, A_4 = 0$, for incident P_s wave,

$A_1, A_2 = 0$, for incident coupled transverse and microrotational wave.

Snell's law is given as

$$\frac{\text{Cos } \theta_0}{V_0} = \frac{\text{Cos } \theta_1}{\lambda_1^{-1}} = \frac{\text{Cos } \theta_2}{\lambda_2^{-1}} = \frac{\text{Cos } \theta_3}{\lambda_3^{-1}} = \frac{\text{Cos } \theta_4}{\lambda_4^{-1}}, \quad \text{... (24)}$$

where

$$\delta_1 (\lambda_1^{-1}) = \delta_2 (\lambda_2^{-1}) = \delta_3 (\lambda_3^{-1}) = \delta_4 (\lambda_4^{-1}) = kc,$$

$$\text{at } z = 0. \quad \text{... (25)}$$

and

$$V_0 = \begin{cases} \lambda_1^{-1}, & \text{for incident } P_f \text{ wave,} \\ \lambda_2^{-1}, & \text{for incident } P_s \text{ wave,} \\ \lambda_4^{-1}, & \text{for incident coupled transverse and microrotational wave} \end{cases}$$

Making use of potentials given by equation (23) and the Snell's law given by equation (24), the boundary conditions (22) reduce to a system of four non-homogeneous equations represented as

$$\sum_{j=1}^{4} a_{ij} z_j = b_i, \ (i = 1, \ ..., \ 4) \quad \text{... (26)}$$

where

$$a_{1i} = [\lambda + Q \mu_i + (2\mu + K) \sin^2 \theta_i] \delta_i^2, \ i = 1, \ 2,$$

$$a_{1j} = -(2\mu + K) \cos \theta_j \sin \theta_j \delta_j^2, \ j = 3, \ 4,$$

$$a_{2i} = (2\mu + K) \cos \theta_i \sin \theta_i \delta_i^2, \ i = 1, 2,$$

$$a_{2j} = (\mu + K) \delta_j^2 \sin^2 \theta_j - \mu \delta_j^2 \cos^2 \theta_j + K\mu_j, \ j = 3, \ 4,$$

$$a_{31} = a_{32} = a_{43} = a_{44} = 0,$$

$$a_{3j} = \mu_j \delta_j \sin \theta_j, j = 3, 4,$$

$$a_{4i} = (Q + \mu_i R)\, \delta_i^2 , \quad i = 1, 2 \qquad \ldots (27)$$

and $b_i = (i = 1, \ldots, 4)$ are given as follows :

(i) For an incident P_f wave

$$b_1 = -a_{11}, b_2 = a_{21}, b_3 = a_{31}, b_4 = -a_{41}.$$

(ii) For an incident P_s wave

$$b_1 = -a_{12}, b_2 = a_{22}, b_3 = a_{32}, b_4 = -a_{42}.$$

(iii) For an incident coupled transverse and micro rotational wave

$$b_1 = a_{14}, b_2 = -a_{24}, b_3 = a_{34}, b_4 = a_{44}. \qquad \ldots (28)$$

The amplitude ratios of various reflected waves are

$$z_j = \frac{B_j}{A'}, \quad j = 1, \ldots, 4. \qquad \ldots (29)$$

where

$$A' = \begin{cases} A_1, & \text{for incident } P_f \text{ Wave} \\ A_2, & \text{for incident } P_s \text{ wave} \\ A_4, & \text{for incident coupled transverse and microrotational wave.} \end{cases}$$

and $z_j\, (j = 1, .. 4)$ are the amplitude ratios for the reflected P_f wave at an angle θ_1, reflected P_s wave at an angle θ_2, the reflected coupled transverse and microrotational waves at angles θ_3 and θ_4 respectively.

PARTICULAR CASES

Case I — Neglecting porous effect, our results reduce in micropolar elastic solid half-space as

$$\sum_{j=1}^{3} a'_{ij}\, z_j = b_i, \quad i = 1, 2, 3, \qquad \ldots (30)$$

where

$$a'_{11} = [\lambda + (2\mu + K) \sin^2 \theta_2]\, \delta_2'^2 ,$$

$$a'_{12} = -(2\mu + K) \cos \theta_3 \sin \theta_3\, \delta_3'^2 , \quad a'_{13} = -(2\mu + K) \cos \theta_4 \sin \theta_4\, \delta_4'^2 ,$$

$$a_{21}' = (2\mu + K)\cos\theta_2 \sin\theta_2\, \delta_2'^2 ,$$

$$a_{22}' = (\mu + K)\,\delta_3'^2 \sin\theta_3 - \mu\,\delta_3'^2 \cos^2\theta_3 + K\mu_3',$$

$$a_{23}' = (\mu + K)\,\delta_4'^2 \sin^2\theta_4 - \mu\,\delta_4'^2 \cos^2\theta_4 + K\mu_4'$$

and $$a_{31}' = 0,\ a_{32}' = \mu_3'\,\delta_3' \sin\theta_3,\ a_{33}' = \mu_4'\,\delta_4' \sin\theta_4, \qquad \text{... (31)}$$

where

$$\mu_{3,4}' = \frac{\delta_{3,4}'^2\,(\delta_{3,4}'^2 - \omega^2 E_2' - pr_2)}{p[-r_0 + r_1\,\omega^2]},$$

$$\delta_{3,4}'^2 = \omega^2 \lambda_{3,4}'^2,\ \lambda_{3,4}'^2 = [D' \mp (D'^2 - 4E')^{1/2}]/2,$$

$$D' = \frac{1}{C_2^*} + r_1 + \frac{(pr_2 - r_0)}{\omega^2},$$

$$E' = \frac{1}{C_2^*}\left[r_1 - \frac{r_0}{\omega^2} \right],\ C_2^* = \frac{\mu + K}{\rho},$$

$$E_2' = \frac{1}{C_2^*},\ \delta_2'^2 = \omega^2 \lambda_2'^2 , \qquad \text{... (32)}$$

$$\lambda_2'^2 = \frac{\rho}{\lambda + 2\mu + K}$$

and b_i (i = 1, 2, 3) are given as follows :

(i) For an incident longitudinal displacement wave

$$b_1 = -a_{11}',\ b_2 = a_{21}',\ b_3 = a_{31}'.$$

(ii) For an incident coupled transverse and microrotational wave

$$b_1 = a_{13}',\ b_2 = -a_{23}',\ b_3 = a_{33}'. \qquad \text{... (33)}$$

The amplitude ratios of three reflected waves are

$$z_1 = \frac{B_2}{A_0},\ z_2 = \frac{B_3}{A_0},\ z_3 = \frac{B_4}{A_0}, \qquad \text{... (34)}$$

where $A_0 = \begin{cases} A_2, & \text{for incident longitudinal displacement wave,} \\ A_4, & \text{for incident coupled transverse and microrotational wave} \end{cases}$

and $z_j = (j = 1, 2, 3)$ are the amplitude ratios for the reflected longitudinal displacement wave at an angle θ_2, reflected coupled transverse and microrotational waves at angles θ_3 and θ_4 respectively. The above results agree with those obtained by Parfitt and Eringen[14].

Case II — By neglecting micropolar effect, we obtain a system of three non-homogeneous equations in liquid-saturated porous solid half-space as

$$\sum_{j=1}^{3} c_{ij} z_j = b_i, \; i = 1, 2, 3 \qquad \ldots (35)$$

where

$$c_{1i} = [\lambda + Q \mu_i' + 2\mu \sin^2 \theta_i] \delta_i^{*2}, \; i = 1, 2,$$

$$c_{13} = -2\mu \delta_4^{*2} \cos \theta_4 \sin \theta_4,$$

$$c_{2i} = 2\mu \delta_i^{*2} \cos \theta_i \sin \theta_i, \; i = 1, 2,$$

$$c_{23} = \mu \delta_4^{*2} (\sin^2 \theta_4 - \cos^2 \theta_4),$$

$$c_{3i} = (Q + \mu_i' R) \delta_i^{*2}, \; i = 1, 2 \qquad \ldots (36)$$

and $c_{33} = 0$

where

$$\delta_{1,2}^{*2} = \omega^2 \lambda_{1,2}^{*2}, \lambda_{1,2}^{*2} = \frac{B^* \mp (B^{*2} - 4A C^*)^{1/2}}{2A^*},$$

$$\delta_4^{*2} = \omega^2 \lambda_4^{*2}, \lambda_4^{*2} = \frac{C}{\mu \left[\rho_{22} + \frac{ib}{\omega} \right]},$$

$$A^* = PR' - Q^2, \; P' = \lambda + 2\mu, \qquad \ldots (37)$$

$$B^* = P' \left(\rho_{22} + \frac{ib}{\omega} \right) + R \left(\rho_{11} + \frac{ib}{\omega} \right) - 2Q \left(\rho_{12} - \frac{ib}{\omega} \right),$$

$$\mu_{1,2}' = \frac{1}{B'} [-A^* \lambda_{1,2}^{*2} + (\rho_{11} R - \rho_{12} Q) + \frac{ib}{\omega} (R + Q)],$$

and b_i, $(i = 1, 2, 3)$ are given as follows :

(i) For an incident P_f wave

$$b_1 = -c_{11},\ b_2 = c_{21},\ b_3 = -c_{31}.$$

(ii) For an incident P_s wave

$$b_1 = -c_{12},\ b_2 = c_{22},\ b_3 = -c_{32}. \qquad \text{... (38)}$$

(iii) For an incident S_v wave

$$b_1 = c_{13},\ b_2 = -c_{23},\ b_3 = c_{33}.$$

The amplitude ratios z_j, $(j = 1, 2, 3)$ for various reflected waves are given as

$$z_1 = \frac{B_1}{A^*},\ z_2 = \frac{B_2}{A^*},\ z_3 = \frac{B_4}{A^*}, \qquad \text{... (39)}$$

where

$$A^* = \begin{cases} A_1, & \text{for an incident } P_f \text{ wave.} \\ A_2, & \text{for an incident } P_s \text{ wave,} \\ A_4, & \text{for an incident } S_v \text{ wave} \end{cases}$$

and z_j $(j = 1, 2, 3)$ are the amplitude ratios of reflected longitudinal P_f wave at an angle θ_1, reflected longitudinal P_s wave at an angle θ_2 and the reflected S_v wave at an angle θ_4 respectively. The above results agree with those obtained by Deresiewicz and Rice[5].

II RAYLEIGH WAVES IN A MICROPOLAR LIQUID-SATURATED POROELASTIC HALF SPACE

In this case, we assume the solutions in the form

$$q = (A_1 e^{-\zeta_1 z} + A_2 e^{-\zeta_2 z}) e^{i(kx - \omega t)},$$

$$\psi = (\mu_1 A_1 e^{-\zeta_1 z} + \mu_2 A_2 e^{-\zeta_2 z}) e^{i(kx - \omega t)},$$

$$H^* = (A_3 e^{-\zeta_3 z} + A_4 e^{-\zeta_4 z}) e^{i(kx - \omega t)}$$

and

$$\phi_2 = (\mu_3 A_3 e^{-\zeta_3 z} + \mu_4 A_4 e^{-\zeta_4 z}) e^{i(kx - \omega t)}, \qquad \text{... (40)}$$

where

$$\zeta_j = (k^2 - \lambda_j^2 \omega^2)^{1/2},\ j = 1, \ldots, 4. \qquad \text{... (41)}$$

Making use of the potentials given by equation (40) in the boundary conditions (22) and eliminating the unknowns A_1, A_2, A_3 and A_4 from the resulting expressions, we obtain the wave-velocity equation for the Rayleigh waves in a micropolar liquid-saturated poroelastic half-space

as

$$\left(e_1-\frac{e_2 f_1}{f_2}\right)\left(e_3-\frac{e_4\mu_3\zeta_3}{\mu_4\zeta_4}\right)+k^2(2\mu+K)^2\zeta_3\left(1-\frac{\mu_3}{\mu_4}\right)\left(\frac{\zeta_2 f_1}{f_2}-\zeta_1\right)=0, \quad \ldots (42)$$

where

$$e_1=(\lambda+2\mu+K)\zeta_1^2-\lambda k^2+\mu_1 Q(\zeta_1^2-k^2),$$

$$e_2=(\lambda+2\mu+K)\zeta_2^2-\lambda k^2+\mu_2 Q(\zeta_2^2-k^2),$$

$$e_3=(\mu+K)\zeta_3^2+\mu k^2-K\mu_3,\ f_1=(Q+\mu_1 R)(\zeta_1^2-k^2)$$

and $$e_4=(\mu+K)\zeta_4^2+\mu k^2-K\mu_4, f_2=(Q+\mu_2 R)(\zeta_2^2-k^2). \quad \ldots (43)$$

(i) Neglecting the porous effect, the frequency equation in reduced form is similar as obtained by Eringen[9].

(ii) As micropolar constants $\to 0$, we obtain the frequency equation in liquid saturated porous solid as obtained by Tajuddin [15].

NUMERICAL RESULTS AND DISCUSSIONS

Following Gauthier[11], we take the following values of the relevant micropolar constants as

$$\rho=2.19 \text{ gm/cm}^3,\ \gamma=.268\times10^{11} \text{ dyne}$$

$$j=0.196 \text{ cm}^2,\ K=.0149\times10^{11} \text{ dyne/cm}^2$$

$$\omega^2/\omega_0^2=10.$$

Following Yew and Jogi[18] and Fatt[10], the following values of relevant parameters have been taken for

(i) kerosene-saturated sandstone.

$$\rho_1=2.1372 \text{ gm/cm}^3,\ \rho_{11}=1.926137 \text{ gm/cm}^3$$

$$Q=0.07635\times10^{11} \text{ dyne/cm}^2,\ \rho_{12}=-0.002137 \text{ gm/cm}^3$$

$$R=0.0326\times10^{11} \text{ dyne/cm}^2,\ \rho_{22}=0.215337 \text{ gm/cm}^3$$

$$\lambda=.4339\times10^{11} \text{ dyne/cm}^2,\ \mu=.2765\times10^{11} \text{ dyne/cm}^2$$

(ii) water-saturated sandstone

$$\rho_1=2.1712 \text{ gm/cm}^3,\ \rho_{11}=1.9032 \text{ gm/cm}^3$$

$Q = 0.013 \times 10^{11}$ dyne/cm^2, $\rho_{12} = 0.0$ gm/cm^3

$R = 0.0637 \times 10^{11}$ dyne/cm^2, $\rho_{22} = 0.1268$ gm/cm^3

$\lambda = .306 \times 10^{11}$ dyne/cm^2, $\mu = .922 \times 10^{11}$ dyne/cm^2

$$f = \frac{b}{\rho_1 \omega} = 0.712547$$

For the above values of relevant parameters, the system of equations (26) for the amplitude ratios $|z_i|$, (i = 1, . ., 4) are solved by Gauss elimination method for different angles of emergence of the incident P_f (fast P-wave), P_s (slow P-wave) and coupled transverse and microrotational waves starting from grazing incidence ($\theta_0 = 0^0$) to the normal incidence ($\theta_0 = 90^0$). The variations of amplitude ratios for micropolar elastic with liquid-saturated porpous (MEP), elastic with porous (EP) and micropolar elastic (ME) have been shown by solid line (----), small dashed line (.....) and long dashed line (----) respectively. The variations of the amplitude ratios $|z_i|$, (i = 1, .., 4) for MEP and $|z_i|$ (i = 1, 2, 3) for EP and ME with the angle of emergence θ_0 of the incident P_f wave (Figs. 2-5), incident P_s wave (Figs 6-9) and incident coupled transverse and microrotational wave (Figs. 10-13) are shown graphically for kerosene-saturated sandstone.

Case I — Incident P_f Wave.

The amplitude ratio $|z_1|$ for MEP has large values in comparison to $|z_1|$ for EP in the range $0^o \le \theta_0 \le 82^o$ due to micropolar effect but have nearly the same values in the range $83^o \le \theta_0 \le 90^o$, as shown in Fig. 2. In Fig. 3 also, the micropolar effect increases the values of amplitude ratio $|z_2|$ for MEP in comparison to $|z_2|$ for EP in the range $6^o \le \theta_0 \le 72^o$, Fig. 4 shows the variations of the amplitude ratio $|z_3|$ of reflected coupled transverse and microrotational wave for MEP. It is clear from Fig. 5 that due to micropolar effect, the amplitude ratio $|z_4|$ for MEP has large values in comparison to $|z_3|$ for EP in the range $4^o \le \theta_0 \le 42^o$; has small values in the range $43^o \le \theta_0 \le 81^o$ and again has large values in the range $83^o \le \theta_0 \le 90^o$.

Case II — Incident P_s Wave.

In this case also due to presence of micropolar and porous effects, the values of amplitude ratios $|z_1|$, i = 1, . ., 4 for MEP are large in comparison to $|z_i|$, i = 1, 2, 3 for EP and ME theories. Therefore the variations of $|z_i|$, i = 1, . ., 4 for MEP have been shown by multiplying their original values by 10^{-1}. The variations of amplitude ratios $|z_2|$ and $|z_3|$ for ME are shown by multiplying their original values by 10^3 and 10 respectively, so that a comparison between variations of amplitude ratios for MEP, EP and ME theories can be shown graphically simultaneously.

Case III — Incident Coupled Transverse and Microrotational Wave.

Due to presence of micropolar effect, the values of amplitude ratios $|z_1|$ and $|z_2|$ for MEP are small in comparison to $|z_1|$ and $|z_2|$ for EP. Also the porous effect decreases the values of amplitude ratio $|z_2|$ for MEP as shown in Fig. 11. Whereas in figs. 12 and 13, there is no significant effect of micropolar or porous media.

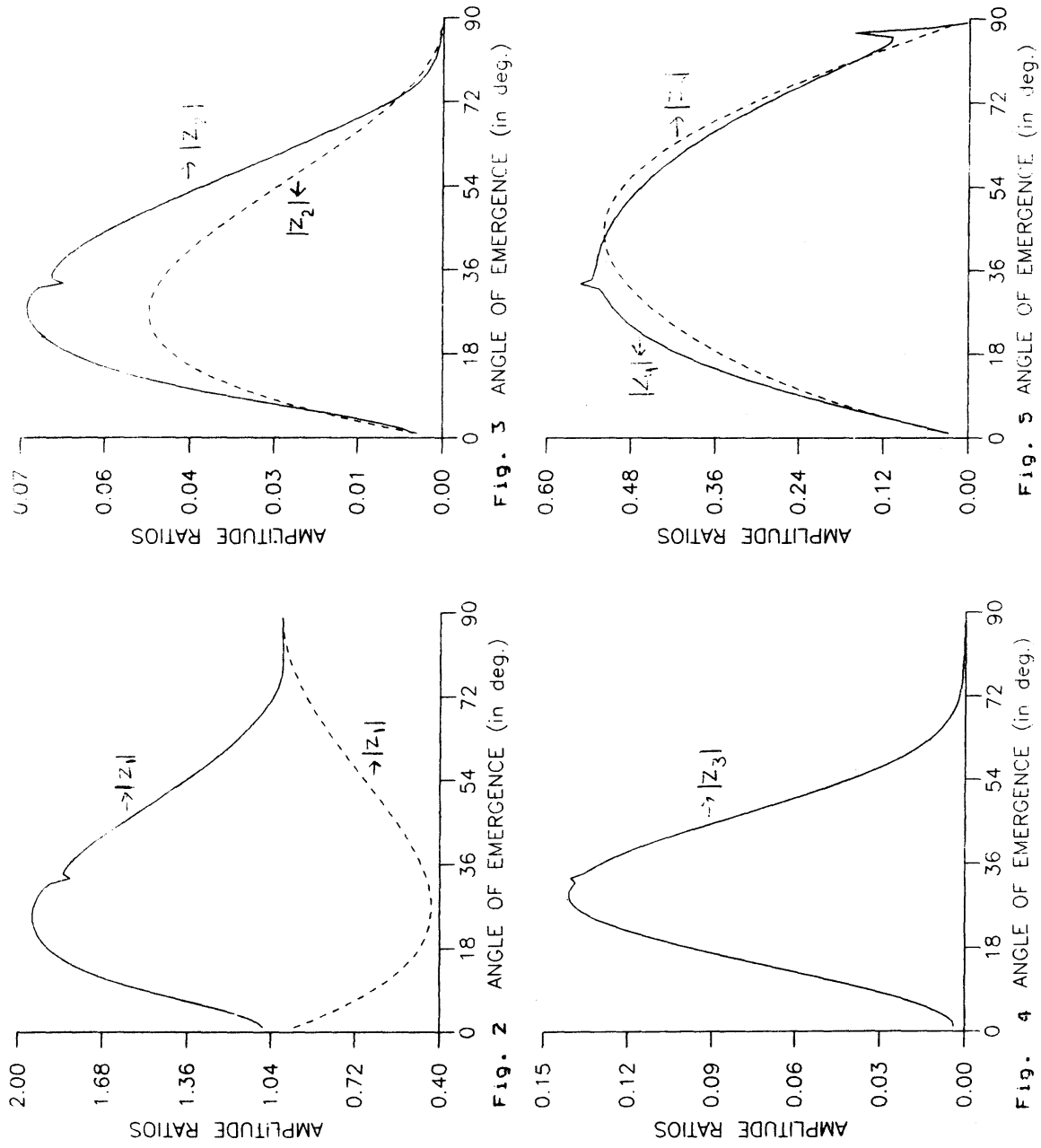

Fig. 2 Fig. 3 Fig. 4 Fig. 5

FIG. 2-5. Variation of amplitude ratios with incident angle of *Ps*-wave

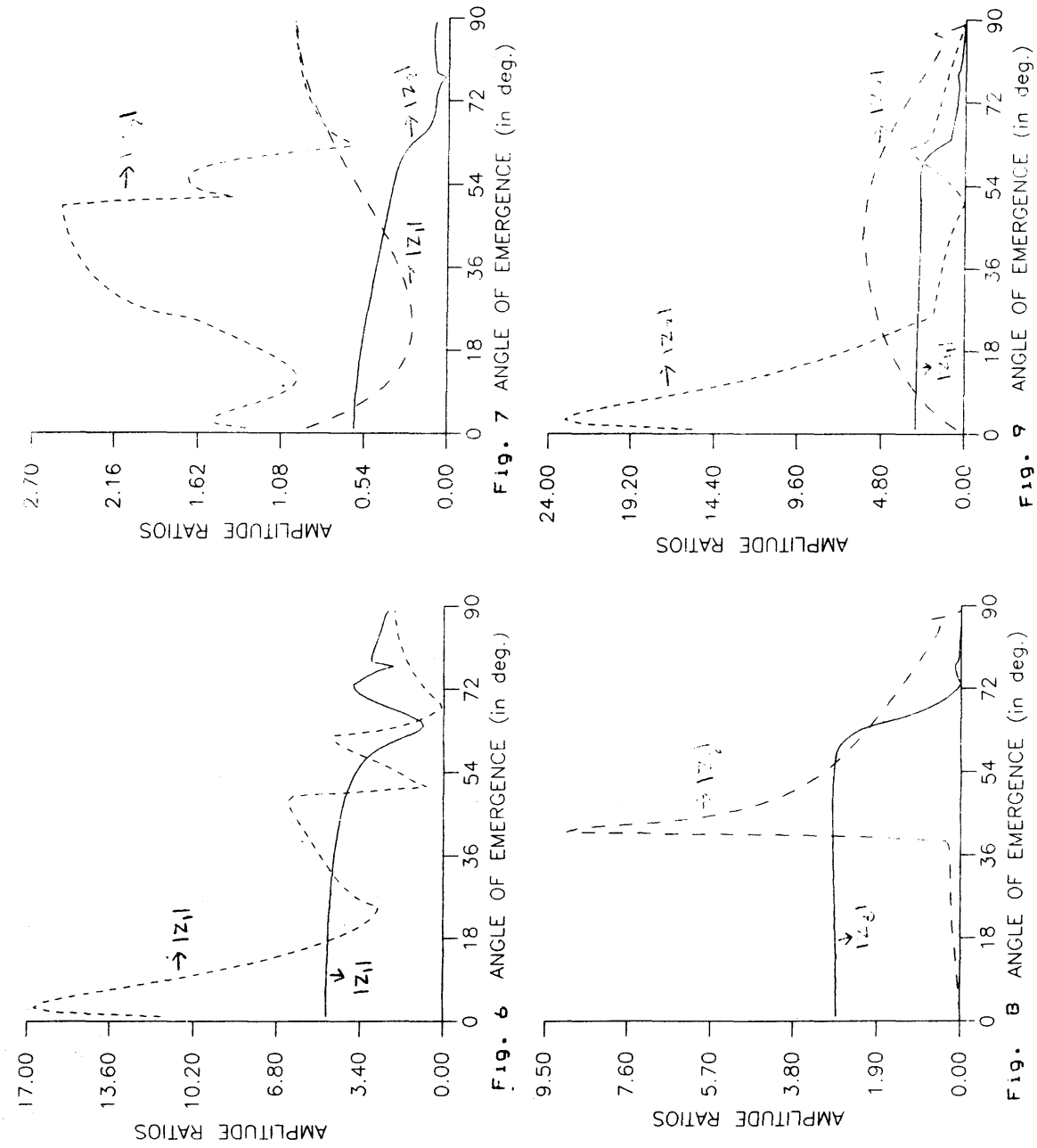

FIG. 6-9. Variation of amplitude ratios with incident angle of P_3-wave

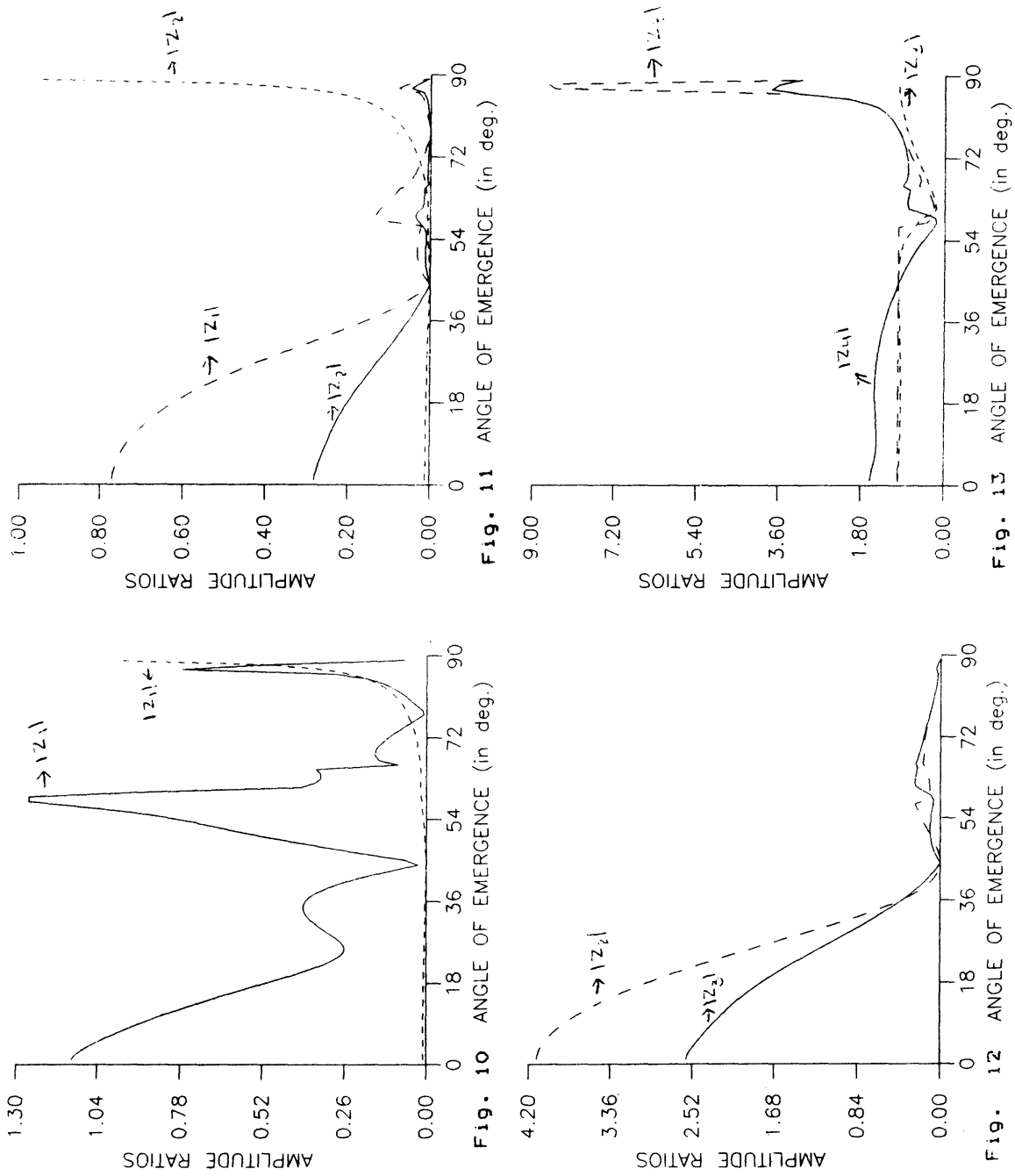

FIG. 10-13. Variation of amplitude ratios with incident angle of coupled wave

As the values of amplitude ratios $|z_i|$, $i = 1, 2$, for EP are large in comparison to $|z_i|$, $i = 1, 2$ for MEP and $|z_1|$ for ME, therefore the variations of $|z_i|$, $i = 1, 2$ for EP have been shown by multiplying the original values by 10^{-2} each; and that of $|z_1|$ for ME is multiplied by 10^{-1}.

Although from Fig. 10, it appears very slight variations in the values of amplitude ratio $|z_1|$ for EP, but it has very effective variations and is depicted in Fig. 10 (a).

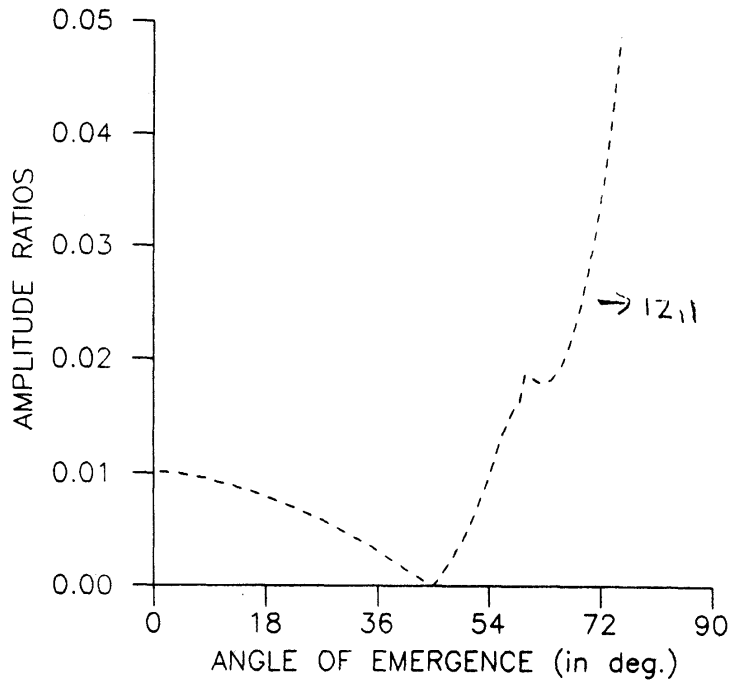

FIG. 10(a). Variations of amplitude ratios with incident angle of coupled wave.

DISCUSSION FOR CASE II

Here we discuss the possibility of propagation of surface waves along the x-direction for kerosene-saturated sandstone and water-saturated sandstone with microstructure as an elastic half space. Equation (42) is a complex equation. For real wave number, it is not possible to find the value of the real wave velocity. This equation has, therefore been reduced to a real equation by assuming that the kerosene-saturated sandstone and water-saturated sandstone is non-dissipative. This is an assumption in order to solve the frequency equation (42) numerically, to obtain the velocity of propagation.

Using the values of parameters as taken in Case I, we obtain the solution of equation (42) for velocity ratio c/C_1^* $(C_1^* = (P/\rho)^{1/2})$, as a function of frequency ratio ω^2/ω_0^2 $(\omega_0^2 = K/\rho j)$ for kerosene-saturated sandstone and normalized wave number kh for (i) kerosene-saturated sandstone and (ii) water-saturated sandstone and these variations are presented graphically in Figs. 14, 15 and 16 respectively. We observe that due to presence of porous medium, the phase velocity for MEP is large in comparison to phase velocity for ME theory and becomes constant after a certain range. For EP, we obtain the Rayleigh root (.51035) for the frequency equation (42). Therefore, it is observed that the frequency equation (42) for MEP and ME theories is dispersive.

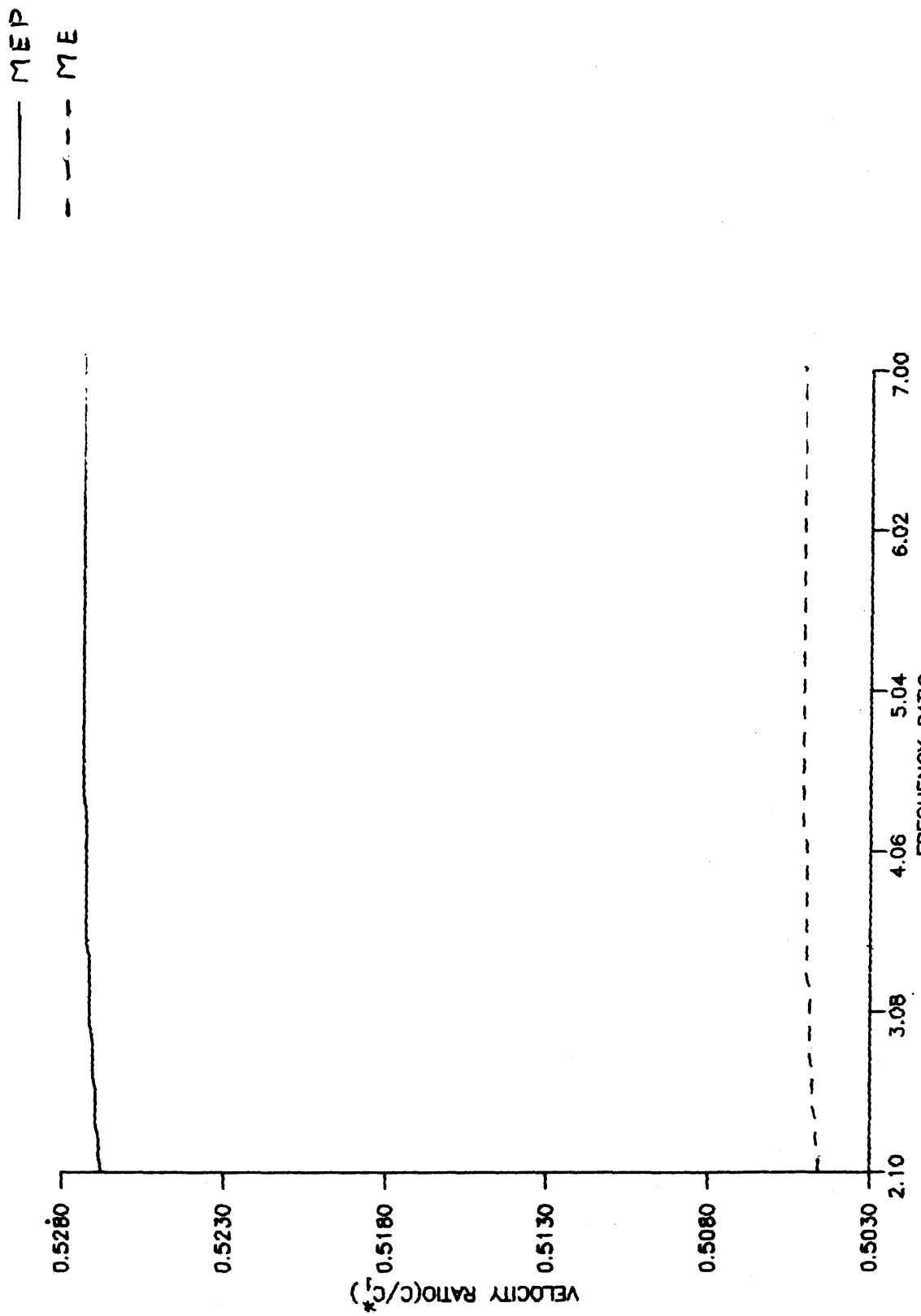

FIG. 14. Dispersion curve of velocity ratio versus frequency ratio

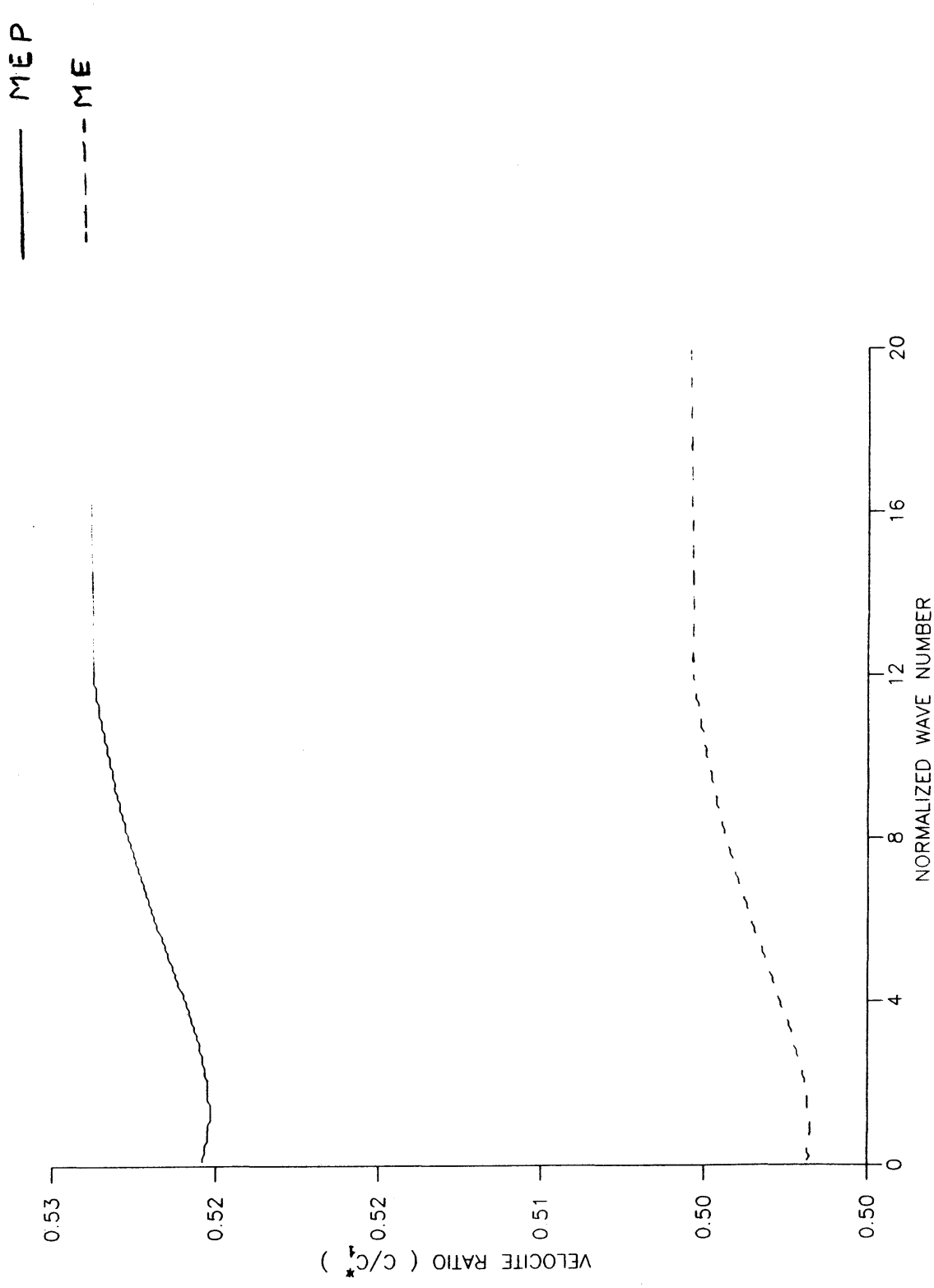

FIG. 15. Dispersion curve of velocity ratio versus normalized wave number

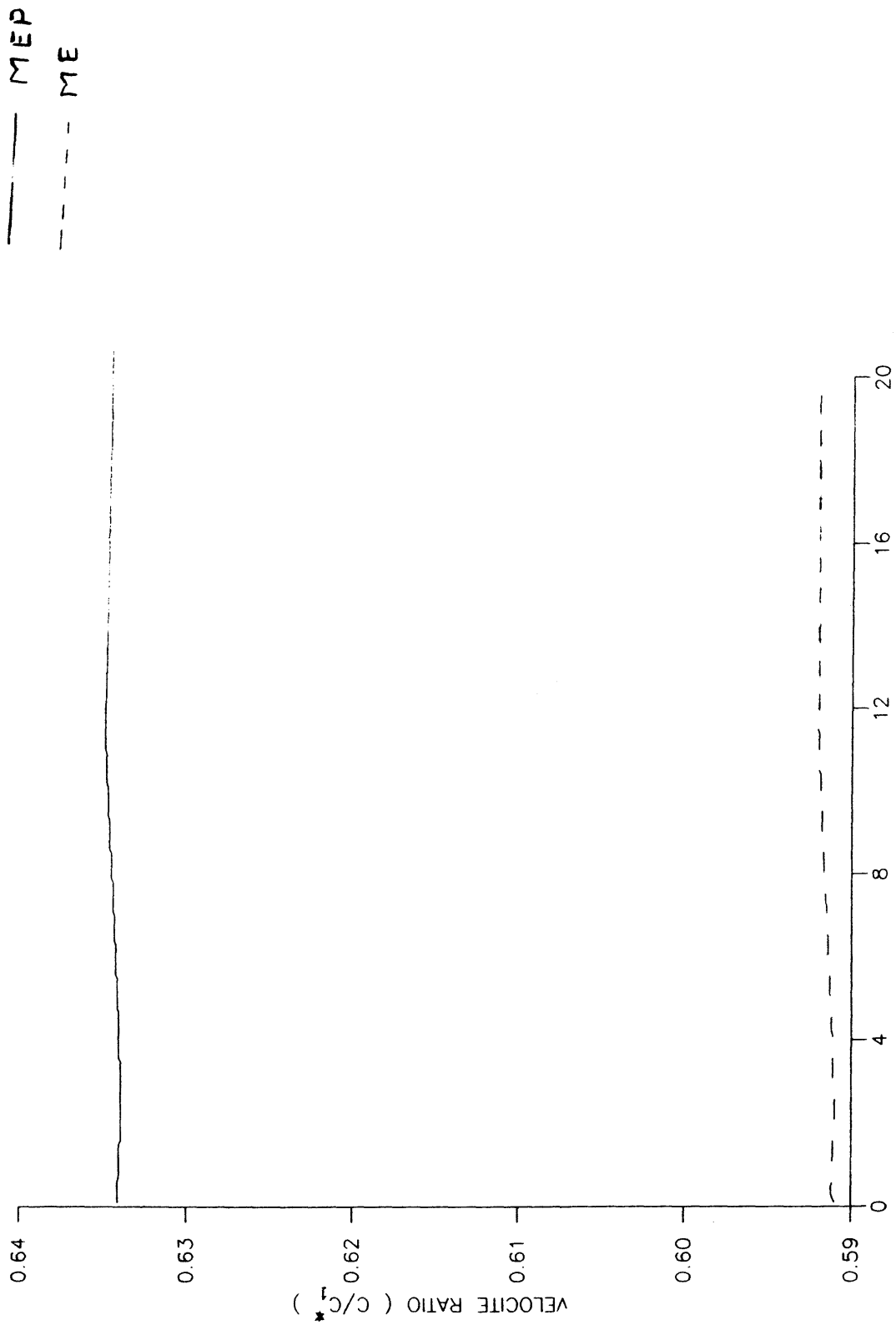

FIG. 16. Dispersion curve of velocity ratio versus normalized wave number

REFERENCES

1. M. A. Biot, *J. appl. Mech.*, **23** (1956), 91-95.
2. M. A. Biot, *J. acoust. Soc. Am.* **28** (1956), 168-191.
3. M. A. Biot, *J. appl. Phys.* **33** (1962), 1482-1498.
4. H. Deresiewicz, *Bull seism. Soc. Am.*, **50** (1960), 599-607.
5. H. Detesiewicz and J. T. Rice, *Bull seism. soc. Am.* **52** (1962) 595-625.
6. A. C. Eringen and E. S. Suhubi, *Int. J. Engng. Sci.*, **2** (1964), 189-203, 389-404.
7. A. C. Eringen, *Proc. XI unt. Congr. appl. Mech.* Springer, Berlin, 1965.
8. A. C. Eringen, *J. math. Mech.*, **15** (1966), 909-923.
9. A. C. Eringen, *Theory of Micropolar Elasticity in Fracture*, Chap. 7 Vol. II, Academic Press, New York, 1968.
10. I. Fatt, *J. appl. Mech.* **26** (1959), 296-297.
11. R. D. Gauthier, *Mechanics of Micropolar Media* (*Ed.* O. Brulin and R.K.T. Hsieh), World Scientific, Singapore. 1982.
12. Z. Konczak, *ZAMM., Z. angew. Math Mech.* **66** (1986) 4, 152-154.
13. Z. Konczak, *ZAMM, Z. angew Math Mech.* **67** (1987) 1, 201-203.
14. V. R. Parfitt and A. C. Eringen, *J. acoust. Soc. Am.*, **45** (1969), No. 5, 1258-1272.
15. M. Tajuddin, *J. acoust. Soc. Am.* **75**(3), (1984), 682-684.
16. S. K. Tomar and M. L. Gogna, *Int. J. Engng. Sci.*, **33** (1995) No. 4 485-496.
17. S. K. Tomar and R. Kumar, *Int. J. Engng. Sci.*, **33** (1995) No. 10, 1507-1515.
18. C. H. Yew and P. N. Jogi, *J. acoust. Soc. Am.* **60** (1976), 2-8.
19. Yang and Lakes, *J. Biomech.*, **15** (1982), 91.